Advances on Ultrafast Silicon Field Emitter Array Photocathodes for Coherent Radiation Sources Based on Inverse Compton Scattering

2014 J. Phys.: Conf. Ser. 557 012055

(http://iopscience.iop.org/1742-6596/557/1/012055)

Advances on Ultrafast Silicon Field Emitter Array Photocathodes for Coherent Radiation Sources Based on Inverse Compton Scattering

C Dong[1], M Swanwick[2], P D Keathley[1], F X Kärtner[1,3] and L F Velásquez-García[2]
[1] Department of Electrical Engineering and Computer Science, Massachusetts Institute of Technology, 77 Massachusetts Avenue, Cambridge, MA 02139, USA
[2] Microsystems Technology Laboratories, Massachusetts Institute of Technology, 77 Massachusetts Avenue, Cambridge, MA 02139, USA
[3] Center for Free-Electron Laser Science, DESY and Department of Physics, University of Hamburg, Notkestralse 85, D-22607, Hamburg, Germany

E-mail: Velasquez@alum.mit.edu

Abstract. Low-cost, compact, and coherent X-rays sources would enable exciting applications such as biomedical imaging of soft tissue and real-time visualisation of molecules at a widespread scale. A promising approach to implement such an X-ray source is based on inverse Compton scattering of a series of nanostructured electron sheets accelerated to relativistic speeds. Photon-triggered field emission arrays can readily produce planar arrays of electron bunches with pC-level sheet charge at high repetition rates using intense laser pulses. In this article, the performance of single-crystal, ultrafast, photon-actuated silicon field emitter arrays is investigated for varying emitter height. Charge vs. incident photon pulse energy characteristics and quantum efficiency of the devices are reported.

1. Introduction

Conventional X-ray imaging is based on absorption, i.e., on registering the spatial change in the intensity of an X-ray beam after passing through the object being imaged [1]. A typical X-ray source for absorption imaging is composed of a thermionic cathode and a reflection anode inside a vacuum chamber with an X-ray transmission window. Electrons emitted by the cathode are accelerated toward the anode using a large bias voltage; deceleration of the electrons in the anode produces X-rays, a mix of bremsstrahlung radiation (broad, continuous spectrum) and fluorescence (emission at specific peaks corresponding to atomic shell transitions of the anode material). A fraction of the X-rays escape the vacuum chamber through a transmission window made of a low-absorption material, e.g., beryllium [2]. X-ray absorption imaging works best in structures made of dense, i.e., high-Z materials, but are not good to image samples made of light, i.e., low-Z materials. For imaging low-Z materials, far greater contrast would be attained if, instead of measuring the relative attenuation of the X-ray beam after passing through the sample, the change in phase of the photons is tracked [3]. Applications of coherent X-ray sources include biomedical imaging, cancer treatment, protein nanocrystallography, and real-time imaging of molecules. In order to be possible phase contrast imaging, a coherent X-ray source is needed. Current coherent X-ray sources are synchrotrons, very expensive and large particle accelerators; therefore, phase contrast imaging is limited to research and high-end applications.

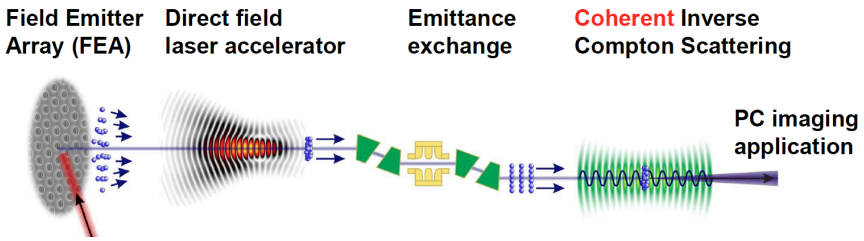

Figure 1. Schematic of the compact coherent X-ray source proposed in [4].

A promising implementation of a low-cost, compact, and coherent X-ray source based on inverse Compton scattering [4] is shown in figure 1. In this approach, a series of nanostructured charge sheets (a planar array of electron bunches) is produced by a photocathode; the sheets are then accelerated to relativistic speeds using an optical field. Then, the charge sheets experience an emittance exchange from the transverse phase space plane into the longitudinal plane (i.e., each sheet, originally advancing in the direction of its normal, now advances in the direction of one of its edges). Finally, a second optical field interacts with the electron bunches, decelerating them and causing coherent X-ray emission. The brilliance and flux of such compact coherent X-ray sources would be similar to those of a synchrotron facility, but with orders of magnitude smaller footprint, power assumption, and cost. A Coherent source based on a laser undulator has been previously proposed [5] but for very different sets of electron beam and laser parameters. In the approach shown in figure 1, the bunch charge and peak current are much lower, as is the electron beam emittance. In addition, the use of a structured electron beam and the exchange of the emittance of the beam results in visibly less number of gain lengths and power consumption, as well as less stringent focusing and pulse length requirements on the laser.

State-of-the-art ultrafast cathodes are flat surfaces that use highly reactive materials to lower the workfunction and increase the quantum efficiency of single-photon absorption of ultraviolet pulses. However, these devices have several disadvantages including (i) they need to be fabricated, stored and operated in ultra-high vacuum, and (ii) production of high current density pulses reduces their lifetime due to the rapid degradation of the low workfunction material [6]. Photon-triggered field emission cathodes are a promising technology to bypass these shortcomings. In these devices, electron tunneling occurs when the electric field of high-intensity optical pulses interacts with field enhancing structures [7]. Most work on ultrafast photo-triggered field emission cathodes has focused on single tips that are serially manufactured. We recently demonstrated batch fabricated photon-triggered field emission cathodes composed of massively multiplexed (> 100,000 tips, 4.6-million tips.cm^{-2}), uniform (<1 nm tip radius standard deviation) arrays of nano-sharp high-aspect-ratio silicon pillars, capable of pC-level emission with multi-kHz repetition [8]. These devices are made using standard CMOS batch fabrication processes, are stored at atmospheric pressure, and can be operated at lower vacuum levels compared to standard photocathodes with no degradation; in addition, the structure of the cathode shapes the emission as a series of planar arrays of electron bunches, which is essential for the coherent X-ray source approach we described. In a recent article we reported the effect of emitter pitch scaling on the performance of the field emitter arrays [9]; in this article we investigate the effect of varying the emitter height on the performance of the field emitter arrays; we provide charge vs. incident laser pulse energy characteristics as well as estimate the quantum efficiency of the cathodes.

2. Device fabrication

To fabricate the devices, an array of coin-like features is formed on a <100> n-Si wafer wafer using a 250 nm-thick chemical vapor deposited (LPCVD) silicon-rich silicon nitride film, projection lithography, and reactive-ion etching (RIE). Then, an array of coin-like features is created on top of the first array using a 500 nm-thick plasma enhanced chemical vapour deposited (PECVD) silicon dioxide film, projection lithography, and RIE; each oxide feature is concentric within 0.1 μm to the nitride feature right underneath. Third, the emitter body is etched using deep reactive-ion etching

(DRIE); the wafers are then cleaned and oxidized. The oxidation step thins the pillars and the nitride features act as a diffusion barrier to form the tips. The oxide and nitride films are removed using wet processing, leaving highly uniform arrays of single-crystal silicon pillars. Finally, the wafers are diced into 22-mm squares. For our experiments we made arrays of emitters with 10 μm emitter pitch, 2, 4, and 8.5 μm emitter height, and 6 nm tip radius. A fabricated device is shown in figure 2.

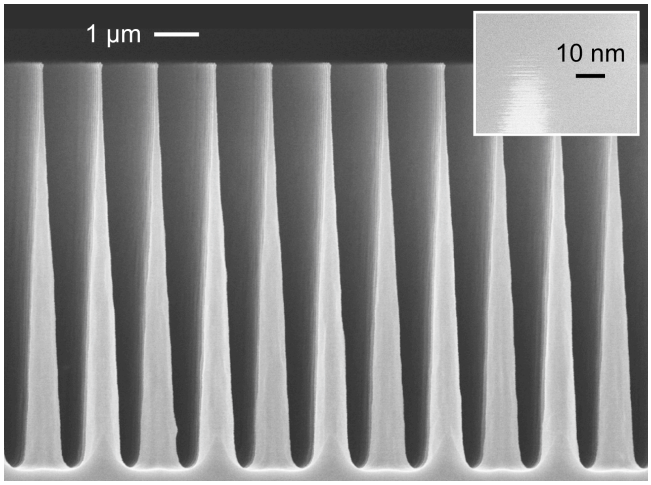

Figure 2. Close-up of an array of electron emitters; each emitter is 8.5 μm tall and the emitter pitch is 1.25 μm.

3. Experimental procedure

An schematic of the photocathode vacuum system is shown in figure 3. The measurement of the charge vs. incident laser energy characteristics takes place in a vacuum chamber with base pressure in the order of 10^{-7}-10^{-8} Torr. The cathode chip is dipped in 2% hydrofluoric acid to remove the native oxide right before characterization and is then connected to ground through a picoammeter (Keithley 6485). The anode electrode, a 0.25" diameter plate, is placed 3 mm above the tips and is connected with a source-measuring unit (SMU: Keithley 237 or Keithley 248), which provides various voltage biases between 10V and 5000 V. The cathode was excited with 35 fs 800nm laser pulses at 3 kHz repetition rate from a regeneratively amplified titanium sapphire oscillator seed. The laser pulses hit the samples at an 84° grazing incidence, creating a 765 μm by 80 μm ellipse. The intensity of the incident wave is controlled by changing the waveplate angle through a LabView script and switching different filter lenses. The data are collected using a LabView script.

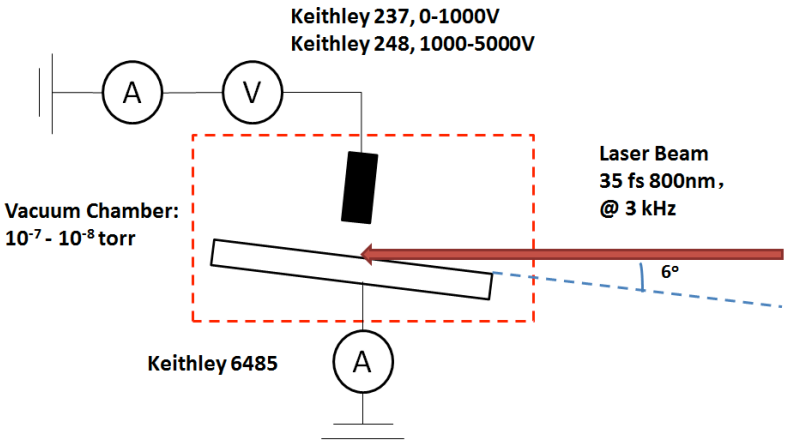

Figure 3. Schematic of the testing rig used to characterize the photocathodes.

4. Experimental results

Figure 4 shows the charge vs. incident laser pulse energy for devices with 10 μm emitter pitch and 2, 4, and 8.5 μm emitter height. At low intensities (<0.3 μJ), an electron absorbs three photons simultaneously in order to escape from the tip surface; this results from silicon's electron affinity (4.05 eV) and the energy of the incident photons (1.55 eV). The slope of the low-energy portion of the characteristics in figure 3 is about 3, consistent with the three-photon absorption process. For larger incident laser pulse intensities (>1 μJ), the optical field bends the barrier that traps the electrons within the tips and electron tunneling occurs. This regime is commonly referred to as the strong-field regime and it follows a time-averaged Fowler-Nordheim model [10]. In this regime, the expected slope of the charge-incident photon energy characteristic is ~1.2 if no space charge effects take place [8]. A slope of 1.06 is obtained in figure 3 for the strong-field regime, in close agreement with the model.

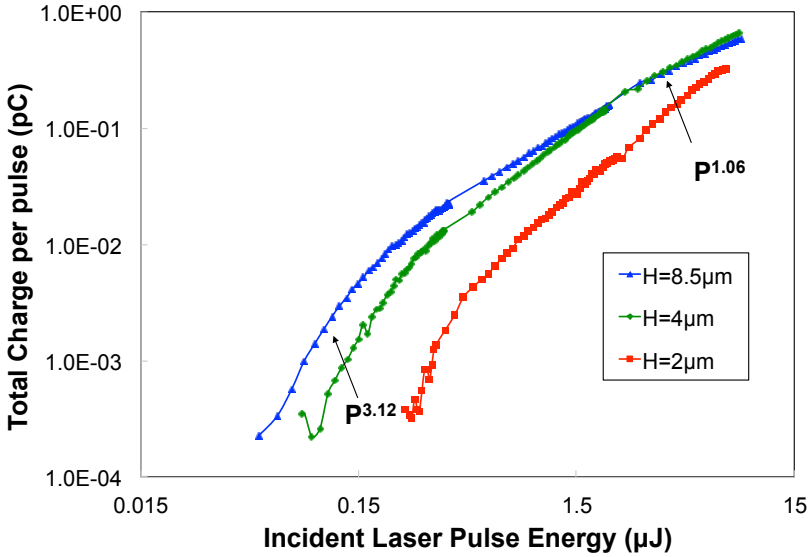

Figure 4. Total emitted charge vs. laser pulse energy for arrays of Si field emitters with 6 nm tip radius, 10 μm pitch and 2 - 8.5 μm height.

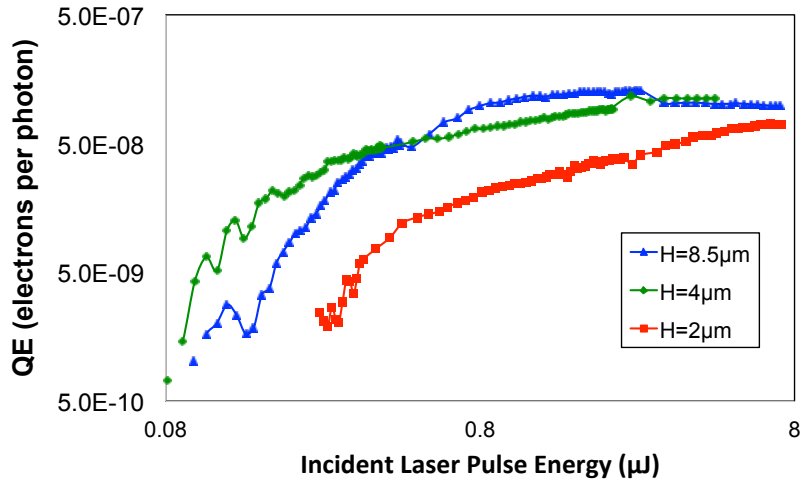

Figure 5. Quantum efficiency versus incident photon energy for arrays of Si field emitters with 6 nm tip radius, 10 μm pitch and 2 - 8.5 μm height.

In figure 4 the charge per incident photon pulse increases for larger the emitter height, as expected from the larger emitter field factor of taller emitters. However, for large enough intensity (>1.5 μJ), the characteristics converge and no further gains in electron emission are observed. There seems to be an optimum height for a fixed emitter pitch to maximize the total current emission. This is an important result given the greater difficulty for making longer emitters compared to making shorter emitters.

We estimated the quantum efficiency (QE) of our devices based on the data shown in figure 4 and the specifications of the laser; the result is shown in figure 5. We observe that in general larger emitter aspect-ratio results in higher QE, although for tall enough emitters and incident photon pulses of enough intensity the QE characteristics converge and become flat. The estimated maximum QE is $\sim 1.3\times10^{-7}$. The QE values are high taking into account that only a very small fraction of the area of the cathode emits electrons, as the emitter tip diameter is about 12 nm and the emitter pitch is 10 μm, resulting in only about a millionth of the area participating in the emission. Nonetheless, the emission is greatly enhanced as compared to that of on planar Si, which has a QE of 10^{-10} [8].

5. Conclusion

We investigated the performance of planar arrays of high-aspect-ratio single-crystal silicon nanosharp electron emitters for varying emitter height. We observed multi-photon emission for low-intensity incident photon pulses (<0.3 μJ), and strong-field emission for high-intensity incident photon pulses (>1 μJ), in agreement with the literature and the models. We observed that the charge emitted per incident photon pulse improves with increasing emitter height; however, for high-intensity incident photons, there is a limit characteristic and no further improvement is perceived. The estimated maximum quantum efficiency at about 1.3×10^{-7} –a high value considering that only about a millionth of the area is involved in the emission process. The quantum efficiency of the devices is better for arrays with taller emitters; however, for incident photon pulses of enough intensity the quantum efficiency characteristic converges and becomes flat.

Acknowledgments

The devices were made at the Microsystems Technology Laboratories of the Massachusetts Institute of Technology. This work was funded in part by the Defense Advanced Research Projects Agency / Microsystems Technology Office, grant N66001-11-1-4192 (Program Manager D Palmer). Any opinions, findings, and conclusions or recommendations expressed in this publication are those of the authors and do not necessarily reflect the views of the US Government and therefore, no official endorsement of the US Government should be inferred.

References

[1] Beckhoff B, Kanngieβer B, Langhoff N, Wedell R, and Wolff H 2006 *Handbook of Practical Xray Fluorescence Analysis* (Berlin: Springer)
[2] Slack C M and Ehrke L F 1941 *J. Appl. Phys.* **12** 165
[3] Donath T, Pfeiffer F, Bunk O, Grünzweig C, Hempel E, Popescu S, Vock P, and David C 2010 *Invest Radiol.* **45** 445
[4] Graves W S, Kärtner F X, Moncton D E, and Piot P 2012 *Phys. Rev. Lett.* **108** 263904
[5] Bacci A, Ferrario M, Maroli C, Petrillo V, and Serafini L 2006 *Phys. Rev. ST Accel. Beams* **9** 060704
[6] Guo Q, Takahashi K, Saito K, Akiyama H, Tanaka T, and Nishio M 2103 *Appl. Phys. Lett.* **102** 092107
[7] Hommelhoff P, Sortais Y, Aghajani-Talesh A and Kasevich M A 2006 *Phys. Rev. Lett.,* **96** 077401
[8] Swanwick M E, Keathley P D, Fallahi A, Krogen P R, Laurent G, Moses J, Kärtner F X, and Velásquez-García L F 2014 *Nano Letters* **14** 5035
[9] Swanwick M E, Dong C D, Keathley P D, Fallahi A, Kärtner F X, and Velásquez-García L F 2014 *Tech. Digest of the 27th Int. Vac. Nanoelectronics Conf., Engelberg, Switzerland, July 6 – 10, 2014,* pp. 69 – 70
[10] Yalunin S V, Gulde M, and Ropers C 2011 *Phys. Rev. B* **84** 195426